

Application of ZnO Nanoparticles in Control of H₂S Emission from Low-Temperature Gases and Swine Manure Gas

Bennet Awume · Mehdi Tajallipour · Mehdi Nemati · Bernardo Predicala

Received: 7 January 2017 / Accepted: 2 March 2017 / Published online: 18 March 2017
© Springer International Publishing Switzerland 2017

Abstract Zinc oxide nanoparticles were evaluated for the removal of hydrogen sulfide from low-temperature gases, as well as swine manure gas using laboratory and semi-pilot scale systems. Effects of gas flow rate (200 and 450 mL min⁻¹), H₂S concentration (90–1500 ppmv), temperature (1–41 °C), and particle size (18, 80–200 nm) were investigated in the laboratory scale system using premixed gases (H₂S-balanced N₂). The breakthrough and equilibrium adsorption capacities increased with an increase of H₂S concentration. Application of high gas flow rates saturated the adsorbent faster and decreased the adsorption capacities. Adsorption capacities of 18 nm particles were higher than those of 80–200 nm. Regardless of H₂S concentration, the equilibrium adsorption capacity was not affected by temperature in the range 1 to 22 °C but increased when a higher temperature of 41 °C was applied. Among the evaluated isotherms, Langmuir-Freundlich described the equilibrium data obtained with 18 and 80–200 nm particles with a higher level of accuracy. Experiments in a semi-pilot scale adsorption system with 18 nm ZnO and gases emitted from the stored swine manure

demonstrated the effectiveness of ZnO nanoparticles in removal of H₂S from these representative gases. Specifically, treatment of manure gas in the semi-pilot scale adsorption system decreased the level of H₂S from an average inlet value of 235.7 ± 85.2 ppmv to a negligible level.

Keywords Manure gas · Hydrogen sulfide · Emission control · Nanoparticles · Adsorption · Semi-pilot scale system

1 Introduction

Hydrogen sulfide (H₂S) is a toxic and corrosive gas which is produced as part of various processes in the petroleum and chemical industries, as well as in livestock operations (Haimour et al. 2005; Sayyadnejad et al. 2008; Tang et al. 2009). In the latter case, bacterial decomposition of sulfur-containing amino acids in the animal excreta results in the formation of H₂S which is then released during manure handling activities such as agitation, transportation, and land application (Curtis 1983; Arogo et al. 2000; Thu 2002; Moreno et al. 2010). Hydrogen sulfide emission is a serious concern due to adverse effects of H₂S on human and animal health, corrosive nature of H₂S, and its contribution to atmospheric acidic depositions.

Physicochemical processes such as Lo-cat, Alkanolamine, Claus, and Holmes as well as bioprocesses have been used to control H₂S emissions in large-scale industrial settings (Tang et al. 2009). In

B. Awume · M. Nemati (✉)
School of Environment and Sustainability, University of Saskatchewan, Saskatoon, SK S7N 5C8, Canada
e-mail: Mehdi.Nemati@usask.ca

M. Tajallipour · M. Nemati
Department of Chemical and Biological Engineering, University of Saskatchewan, Saskatoon, SK S7N 5A9, Canada

B. Predicala
Prairie Swine Centre Inc., Saskatoon, SK S7H 5N9, Canada

livestock operations, application of different additives has been evaluated as a means to control the emission of H₂S (McCrary and Hobbs 2001; Kim et al. 2008; Predicala et al. 2008; Shah et al. 2008; Alvarado et al. 2015). Predicala et al. (2008) reported that the addition of 80 mM Na-nitrite or 2 mM Na-molybdate to manure reduced the level of emitted H₂S from 500 to 2–25 ppmv. A follow-up pilot scale study confirmed the effectiveness of this approach in control of H₂S emission from manure pits (Moreno et al. 2010). Evaluating direct addition of a number of commercially available nanoparticles to the swine manure, Alvarado et al. (2015) reported that ZnO nanoparticles were most effective in reducing emission of H₂S and ammonia (NH₃) from the swine manure. The excessive cost, the need for repeated applications, and more important release of applied nanoparticles with the treated manure are some of the drawbacks associated with direct addition of nanoparticles to manure. Biofiltration has been proven effective in removal of H₂S from contaminated streams (Hartung and Phillips, 1994; Chung et al. 2000; Chang et al. 2004). Chung et al. (2000) used a biofilter with co-immobilized *Thiobacillus thioparus* CH11 and *Nitrosomonas europaea* to treat a mixture of H₂S and NH₃. Removal efficiencies around 95% were achieved for both H₂S and NH₃. Using a mixture of pine chaff and perlite as media in a biofilter, Chang et al. (2004) reported 82.4% decrease in H₂S and odor levels in the treated gas. Excessive pressure drop, necessity for periodic renewal of the filter media and biofilm, and the requirement for skilled operators which collectively translate to high operating costs are some of the disadvantages of biofilters.

Application of tailor-made nanoparticles for the capture of H₂S and other air pollutants has been evaluated in recent years (Rosso et al. 2003; Novochinskii et al. 2004; Li and King, 2006; Wang et al. 2008; Xiao et al. 2008; Simo et al. 2009; Habibi et al. 2010; Nassar and Pereira-Almao, 2010; Song et al. 2013). However, a close look at the existing literature as discussed in details in the latter part of this article reveals that the focus of earlier works has been on the capture of H₂S at high temperatures and information concerning the treatment of ambient temperature gases (e.g., emissions from livestock operations and biogas), specially with metal oxide nanoparticles and representative gases is very limited. Given that an effective, accessible, and easy to use adsorbent with known characteristics would be a preferred option in special applications such as control of

H₂S emission in livestock operations, removal of H₂S by ZnO nanoparticles was evaluated in the present work. Impact of various operating conditions such as temperatures in the ambient range, H₂S concentration, gas flow rate, and particle size was investigated in a laboratory system. The effectiveness of ZnO nanoparticles in capture of H₂S from representative gases was also evaluated in a semi-pilot scale adsorption system using gases emitted from the stored swine manure.

2 Materials and Methods

2.1 Nanoparticles, Premixed, and Swine Manure Gases

ZnO nanoparticles (18 and 80–200 nm) were obtained from the US Research Nanomaterials Inc. (Houston, TX, USA). The BET surface area and pore volume of the particles, determined in this work, were 26.48 m² g⁻¹ and 0.146 cm³ g⁻¹ for 18 nm particles and 11.36 m² g⁻¹ and 0.027 cm³ g⁻¹ for 80–200 nm particles, respectively. Industrial grade nitrogen gas (N₂) and a premixed gas containing 2000 ppmv H₂S-balanced N₂ were used to generate gas streams with different H₂S levels for the laboratory scale experiments (Praxair Canada Inc., Saskatoon, Canada).

Considering the compositional differences of premixed gas and those emitted in livestock operations (i.e., air vs nitrogen as bulk gas, presence of other manure gases and moisture) and to assess the performance of the system in practical situations, additional experiments were conducted in a semi-pilot scale adsorption system using gases emitted from stored swine manure. The manure was collected from the pit of a grow-finish room in the swine barn at the Prairie Swine Centre Inc. (Saskatoon, SK, Canada). Manure slurry was mixed in the pit prior to collection using a mechanical agitator. This allowed resuspension of the settled solids and minimized the variability in manure composition. The mixed slurry was then transferred to eight cylindrical containers (65 L each). Each container was partially filled with 30 L of manure slurry, capped, and left undisturbed at 20 °C for 3 weeks to allow formation and accumulation of H₂S. An outlet sleeve was devised on the container lid that allowed the connection of a flexible rubber tubing and withdrawing the headspace gas during the experiments. The lid also had an air inlet tube which was left open during the experimental runs,

allowing flow of air into the container and replacing the withdrawn gases.

2.2 Laboratory and Semi-Pilot Scale Experimental Systems

The laboratory setup, shown in Fig. 1, consisted of a glass adsorption column ($D = 10$ mm and $H = 150$ mm) with a circulating water jacket and associated water bath (VWR International, Canada), control valves, digital mass flow controllers (Aalborg, New York, USA), tubing with the devised sampling ports, differential pressure transducer (Omega, Stamford, USA), thermocouple (Omega K type, Stamford, USA), and a scrubbing container with 1 M NaOH solution for removing residual H_2S from the exhaust gas. Thin layers of glass wool were placed near the bottom and the top of the adsorption column to support the nanoparticles and to prevent their carryover by the flowing gas. Sufficient space was provided between the bottom and top ends to allow fluidization of particles during the experiments. Gas flow rate was regulated using swing valves and mass flow controllers. Tygon tubing was used to connect various components of the system. Water or a mixture of ethylene glycol and water was used in the water bath to control the temperature of adsorption column. Temperature was monitored by inserting a thermocouple in the upper part of the adsorption column where it was in contact with the gas and fluidized particles. Pressure drop across the column was measured using a differential pressure transducer. Gas samples (500 – 1000 μL) were collected through the sampling ports at designated time intervals using a gastight syringe. The sampling

intervals were 2–3 min at the early stage and 10–15 min after H_2S breakthrough. Syringe was flushed twice with the flowing gas before collecting the gas sample. Samples were analyzed for H_2S content using a gas chromatograph. Sampling syringe was replaced after two to three experimental runs to ensure the accuracy of sample volume. The experimental setup was mounted inside a walk-in fume hood. Personal H_2S monitoring device was worn by the personnel involved. Prior to each experiment, a thorough leak test was performed on the system using nitrogen gas.

The semi-pilot scale experimental setup, shown in Fig. 2, consisted of a transparent PVC adsorption column ($D = 7.5$ cm and $H = 25$ cm) and a centrifugal fan (Keho, Edwards group, Lethbridge, AB) to flow the headspace gas from the manure containers into the adsorption column. Flexible rubber tubing ($D = 10$ cm) was used to connect the manure container to the inlet of the adsorption column and a galvanized duct ($D = 10$ cm) connected the centrifugal fan inlet to the outlet of the column. Results of laboratory experiments showed the superiority of 18 nm ZnO particles; hence, adsorption column was charged with 18 nm ZnO nanoparticles (68.5 g). To hold the nanoparticles and to prevent their carryover by flowing gas filter screens composed of a metallic mesh, a layer of spherical beads (diameter = 0.6 cm) and glass wool were placed near the bottom and the top of the adsorption column. Gas sampling ports with rubber septum were devised at the inlet and outlet of the adsorption column. Gas flow rate was controlled through adjustment of a damper in the fan exhaust line. The superficial velocity of the gas was measured near the column inlet using a port devised in

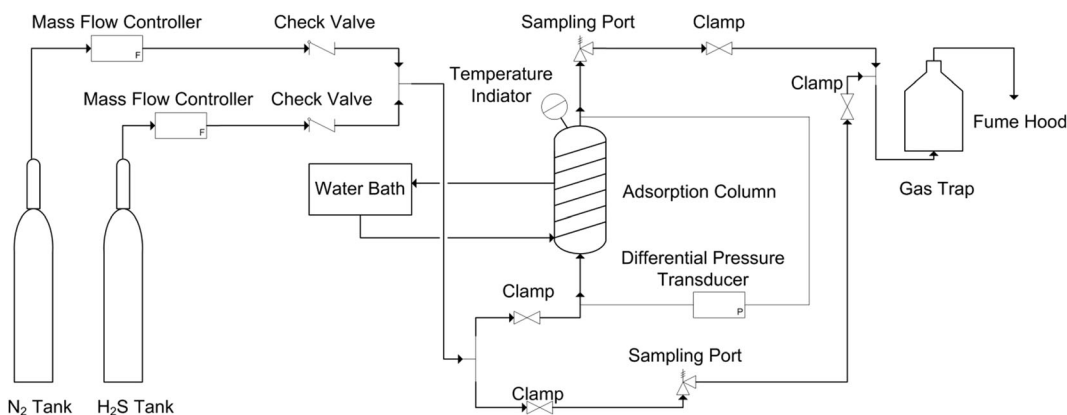
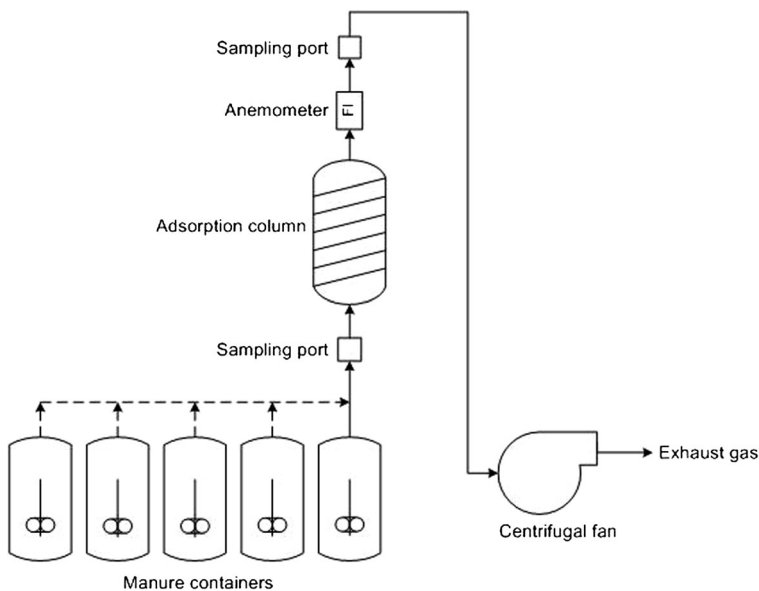


Fig. 1 Schematic diagram of the laboratory experimental setup

Fig. 2 Schematic diagram of the semi-pilot scale experimental setup



the galvanized duct and a thermal anemometer (VelociCalc 9545-A, TSI Inc., Shoreview, MN, USA; accuracy = $\pm 5\%$). The flow rate of the gas was calculated as the product of gas velocity and cross-sectional area of the duct.

2.3 Laboratory Scale Experiments

The effect of H_2S concentration was investigated with feed gas containing ~ 90 to 1500 ppmv H_2S . The concentration range evaluated in this work exceeded the levels normally observed in livestock facilities that are close or lower than 500 ppmv (Chénard et al. 2003; Predicala et al. 2008). Evaluating a wide range, however, allowed us to assess the potential of ZnO nanoparticles for other applications where higher H_2S concentrations are encountered. To achieve the desired H_2S concentrations, the premixed gas (2000 ppmv H_2S -balanced N_2) was diluted with pure nitrogen gas, using mass flow controllers to adjust the flow of each gas to the required rate. A bypass line with sampling port was used to monitor the concentration of the diluted gas before its entrance into the column. Experiments were conducted with 1 g ZnO nanoparticles (18 or 80 – 200 nm) at a constant gas flow rate of 200 ± 0.2 mL min^{-1} at 22 ± 1 °C. Effect of gas flow rate was investigated through an additional experimental run with a gas flow rate of 450 ± 0.3 mL min^{-1} . H_2S concentration, temperature, and adsorbent size and quantity and in this run

were 200 ppmv, 22 ± 1 °C, 18 nm, and 1 g, respectively.

The effect of temperature was evaluated by conducting experiments at 1 , 10 , and 41 °C. These together with experiment at room temperature (22 ± 1 °C) covered the temperature range that likely prevail in applications such as control of emissions from livestock operations and in treatment of biogas. Experiments at 10 °C covered H_2S concentrations in the range 90 to 1500 ppmv to allow comparison with the results obtained at room temperature, while an H_2S concentration of 541 ± 4.2 ppmv was used in the experiments at 1 and 41 °C. All experiments were conducted with 18 nm particles at a gas flow rate of 200 ± 0.2 mL min^{-1} .

Data generated in the laboratory scale system and Eq. 1 were used to determine the breakthrough and equilibrium adsorption capacities of nanoparticles.

$$q = \frac{QC_0}{M} \int_0^t \left(1 - \frac{C}{C_0}\right) dt \quad (1)$$

where q is adsorption capacity (mg H_2S g^{-1}), t is time (min; breakthrough point or saturation point), M is the quantity of adsorbents (g), Q is the gas flow rate (L min^{-1}), and C_0 and C are inlet and outlet concentrations of H_2S (mg L^{-1}), respectively. The breakthrough time was defined as the time when the ratio of H_2S concentrations in the effluent (C) and influent (C_0) approached ~ 0.05 . Equilibrium conditions were

assumed when the breakthrough curve leveled off and concentration of H₂S in the effluent changed by less than 10%. MATLAB Software (R2013a, MathWorks, USA) was used to carry out the required integration.

2.4 Semi-Pilot Scale Experiments

To investigate the effectiveness of ZnO nanoparticles in removal of H₂S from representative gases, semi-pilot scale adsorption system was fed continuously with the gases emitted from stored swine manure for an extended period of 100 min. The required gas stream was generated using five manure containers in sequence whereby each container provided the representative gas for 20 min (five cycles). In each cycle, a manure container was agitated intermittently (2 min agitation at 5 min intervals) during which centrifugal fan withdrew the headspace gas and passed it through the adsorption column. Following this, the next container was connected to the feed line and the cycle was repeated. This approach replicated H₂S concentration profiles that are encountered in swine confinement buildings during manure agitation and draining of manure pits whereby high levels of H₂S are experienced for a short period, followed by a decline in H₂S concentration due to exhaustion of manure H₂S content and ventilation. The centrifugal fan was started immediately after agitation of the first container and provided a gas flow rate of 25 L s⁻¹. Visual observation during the blank tests conducted with air had shown that this flow rate was sufficient to fluidize the nanoparticles without carryover. Gas samples were collected from the inlet and outlet sampling ports at 5 min intervals, with the first set of samples were taken 2 min after initiation of the experiment. Duplicate samples were taken at selected intervals during each run (two to three times) to determine the data variation. A 20-mL gastight syringe was used for collecting the gas samples. Samples were immediately transferred into sampling tubes which were maintained under reduced pressure and brought to the laboratory for analysis. Larger volumes of gas samples were also collected into 10-L Tedlar bags with a septum-embedded cap (SKC Inc., Eighty Four, PA, USA) in three to four sampling events. This allowed the comparison of the data from the small and large volume samples and to ensure

samples taken during the experiments were representative.

Results reproducibility was assessed by conducting a second experimental run in the semi-pilot scale system. Two manure containers were used sequentially in this run, with each container providing feed gas for 25–30 min. Sampling of the inlet and outlet gases was carried out in 3–5 min intervals following the initiation of the experiment. Other experimental conditions, procedures, and analysis were similar to those described earlier. Finally, a control run was carried out in the absence of nanoparticles (i.e., empty adsorption column) to verify the extent of H₂S adsorption by the components of experimental setup (i.e., metallic mesh, glass wool, column, and tubings). All other conditions were similar to those described for the experiments with nanoparticle. It should be pointed out that during the semi-pilot scale runs nanoparticles were neither regenerated nor substituted with the fresh particles.

2.5 Analyses

Concentration of H₂S was determined using a Varian CP-3800 Gas Chromatograph (GC), equipped with a pulsed flame photometric detector (PFPD) and a capillary column (GS-GasPro 30 m × 0.32 mm I.D., Agilent Technologies). The details of operating conditions and calibration procedure are given elsewhere (Moreno et al. 2010). Occasionally, two or three samples were taken simultaneously to determine the uncertainty associated with the analysis. Standard deviations of these data were presented as error bars. Standard gas with known H₂S concentration was injected to GC before, during, and after each experimental run to verify the accuracy of the analysis; when necessary, GC was recalibrated. Some experimental runs were repeated to ensure the reproducibility of the results. The BET surface area and pore volume of nanoparticles were determined using a Micromeritics ASAP 2020 surface area and porosity analyzer (Micromeritics, GA, USA).

2.6 Adsorption Isotherms

As indicated earlier, experimental data obtained in the laboratory system were used to determine the equilibrium adsorption capacity as a function of gas phase H₂S concentration (partial pressure), using Eq. 1. The resulting data were then fitted into Langmuir,

Freundlich, and Langmuir-Freundlich isotherms, described by Eqs. 2, 3, and 4, respectively (Tien 1994):

$$q = \frac{q_s K P}{1 + K P} \quad (2)$$

$$q = K P^{1/n} \quad (3)$$

$$q = \frac{q_s K P^{1/n}}{1 + K P^{1/n}} \quad (4)$$

where q represents the equilibrium adsorption capacity (mg H₂S (g adsorbent)⁻¹) and P denotes H₂S partial pressure (kPa). The remaining parameters q_s (maximum adsorption capacity, mg H₂S (g adsorbent)⁻¹), K , and n are the isotherm coefficients. The coefficients for each isotherm were determined by fitting the experimental data into the isotherm expression. MATLAB Software (R2013a, MathWorks, USA) was used to carry out the required nonlinear regressions.

3 Results

3.1 Effects of H₂S Concentration and Particle Size

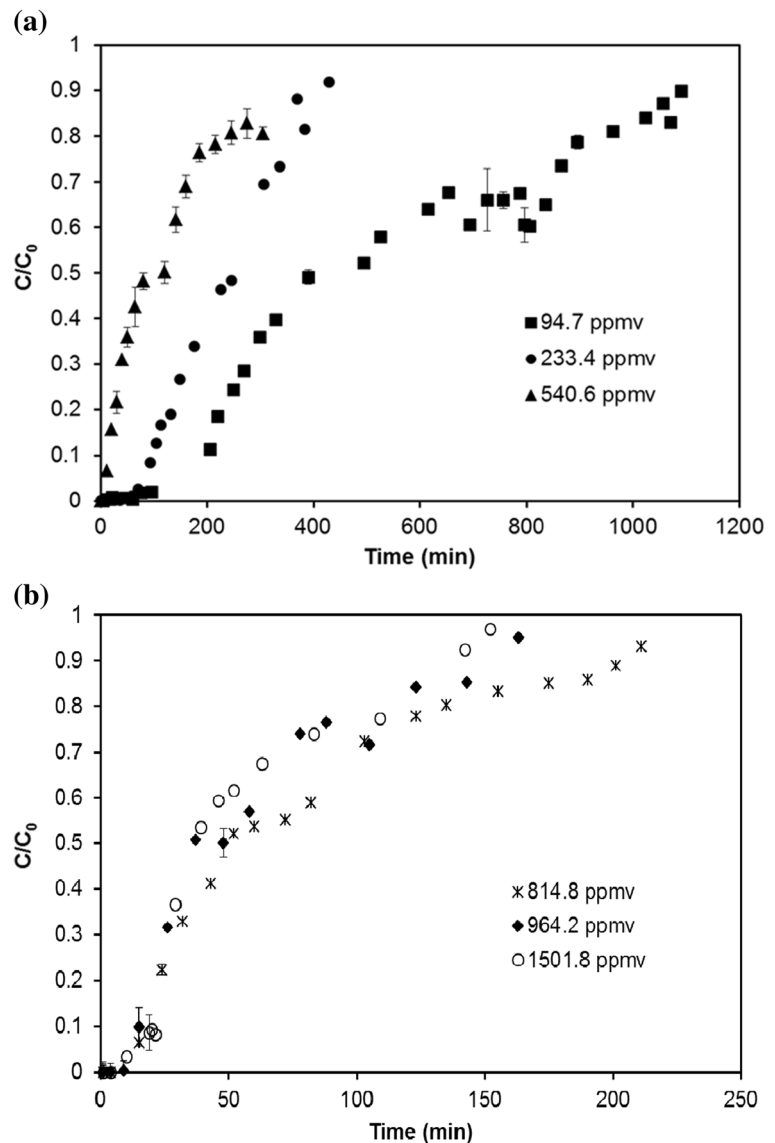
Figure 3 shows the breakthrough curves for adsorption of 94.7 to 1501.8 ppmv H₂S by 18 nm ZnO particles for a gas flow rate of 200 ± 0.2 mL min⁻¹ at 22 ± 1 °C. As seen in Fig. 3a, the breakthrough curves became steeper as feed H₂S concentration was increased from 94.7 to 540.6 ppmv that could be interpreted as an increase in adsorption rate or the rate by which nanoparticles reached their saturation state (Simo et al. 2009). This was also evident from the breakthrough time that showed a decreasing trend with the increase of H₂S concentration, with corresponding breakthrough times for feed H₂S concentrations of 94.7, 233.4, and 540.6 ppmv H₂S, being ~133, 80, and 7 min, respectively. Enhancement in mass transfer driving force due to the increase of H₂S concentration could be the likely reason for this observed pattern. Data presented in Fig. 3b reveals that further increase in H₂S concentrations from 814.8 to 1501.8 ppmv did not have a marked effect (i.e., breakthrough time and slope of breakthrough

curve did not change with the increase of H₂S concentration). Monitoring the temperature indicated that the bed temperature did not change during these experiments (temperature variation <0.5 °C). Pressure drop along the column was also low in all experimental runs (average value = 4.53 ± 1.33 kPa m⁻¹).

Repeated runs (triplicate) were conducted with 964.2 and 1501.8 ppmv H₂S, and analyses of the resulting data revealed that the maximum standard deviation of $\frac{C}{C_0}$ in these runs were 0.19 and 0.09, respectively. Using the experimental data and Eq. 1, the breakthrough and equilibrium adsorption capacities at H₂S concentrations of 94.7, 233.4, 540.6, 814.8, 964.2, and 1501.8 ppmv were calculated as 3.5, 5.1, 1.0, 1.8, 3.0, and 6.7 mg H₂S (g adsorbent)⁻¹ and 14.6, 16.2, 18.8, 17.8, 17.0, and 25.2 mg H₂S (g adsorbent)⁻¹, respectively. Rosso et al. (2003) evaluated the effectiveness of synthesized ZnO with a particles size of 0.34 μm for the removal of 100 ppmv H₂S at a gas flow rate of 400 mL min⁻¹ and 250 °C. Among the synthesized adsorbents, ZnO300 and ZnO400 (numbers indicate calcination temperatures) showed maximum breakthrough adsorption capacities of 33.5 and 26.1 mg H₂S (g adsorbent)⁻¹ and equilibrium adsorption capacities around 51 mg H₂S adsorbed (g adsorbent)⁻¹. Rosso et al. (2003) identified the internal mass transfer as the limiting step in the overall adsorption process.

The effect of particle size was evaluated by conducting experiments with 80–200 nm ZnO particles under conditions similar to those applied with 18 nm particles. Figure 4a, b presents representative sets of data comparing the breakthrough curves obtained with 18 and 80–200 nm particles at H₂S concentrations of 86.8 ppmv (80–200 nm particles) and 94.7 ppmv (18 nm particles) and for H₂S concentrations of 1523.5 ppmv (80–200 nm particles) and 1501.8 ppmv (18 nm particles). As seen in Fig. 4, the breakthrough curves were steeper for larger nanoparticles and particles reached their saturation state faster than their smaller counterpart. This trend was prevalent regardless of H₂S concentration (data only shown for two H₂S concentrations as the others followed the same pattern). The breakthrough capacities for 80–200 nm ZnO particles at H₂S concentrations of 86.8, 202.4, 345.1, 515.8, 1033.3, and 1523.6 ppmv H₂S were 0.1, 0.2, 0.2, 0.5, 0.3, and 0.5 mg H₂S (g adsorbent)⁻¹, respectively, and were generally lower than those obtained with 18 nm particles. The equilibrium adsorption capacity with 80–200 nm ZnO particles was also lower than those for 18 nm particles, with the values for H₂S feed concentration in the range

Fig. 3 Breakthrough curves for H_2S adsorption on 18 nm ZnO nanoparticles. **a** 94.7, 233.4, and 540.6 ppmv H_2S . **b** 814.8, 964.2, and 1501.8 ppmv H_2S . Gas flow rate = $200 \pm 0.2 \text{ mL min}^{-1}$. Temperature = $22 \pm 1 \text{ }^\circ\text{C}$. Error bars represent standard deviation associated with the data determined through repeated sampling and analysis



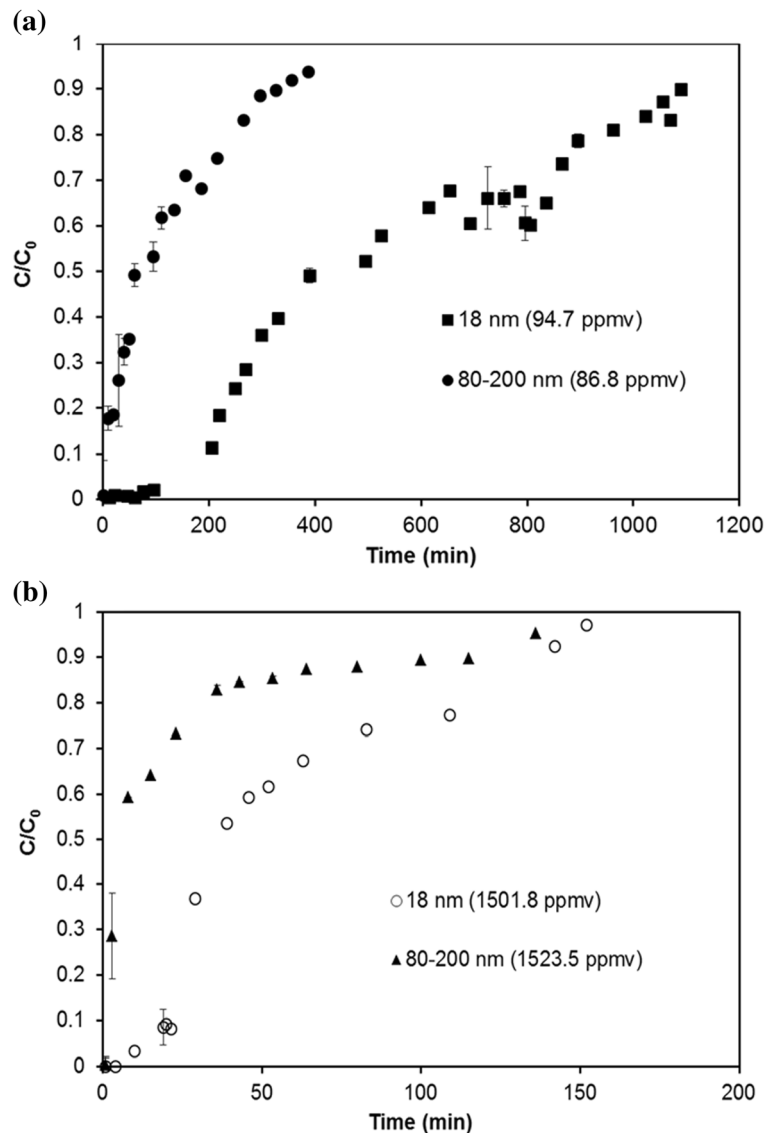
86.8–1523.6 ppmv H_2S being $3.3\text{--}13.8 \text{ mg H}_2\text{S (g adsorbent)}^{-1}$. The observed particle size effect is consistent with the fact that the specific surface area of $80\text{--}200 \text{ nm}$ particles ($11.36 \text{ m}^2 \text{ g}^{-1}$) was lower than that of 18 nm particles ($26.48 \text{ m}^2 \text{ g}^{-1}$) and consequently large nanoparticles reached their saturation state faster and offered lower adsorption capacities. Novochinskii et al. (2004) investigated the effect of particle size on the H_2S adsorption capacity of ZnO ($0.05\text{--}3 \text{ mm}$) and reported an increase in the breakthrough adsorption capacity due to a decrease of the particle size from 3 to $0.11\text{--}0.15 \text{ mm}$. Further decrease of particle size to $0.05\text{--}0.07 \text{ mm}$ did not have any effect. These authors reported a maximum

breakthrough capacity of $30 \text{ mg H}_2\text{S (g adsorbent)}^{-1}$ for $0.11\text{--}0.15 \text{ mm}$ particles and concluded that the adsorption of H_2S on ZnO was likely limited by diffusion.

3.2 Effect of Temperature

Figure 5 shows the effect of temperature on the adsorption of $541.4 \pm 4.3 \text{ ppmv H}_2\text{S}$ (panel a), and $1567.8 \pm 63.0 \text{ ppmv H}_2\text{S}$ (panel b) by 18 nm ZnO nanoparticles at a gas flow rate of $200 \pm 0.2 \text{ mL min}^{-1}$. Temperature in the range $1\text{--}41 \text{ }^\circ\text{C}$ did not have a marked effect on the breakthrough time or the slope of breakthrough curves, specially with $541.4 \pm 4.3 \text{ ppmv H}_2\text{S}$, where the values of breakthrough

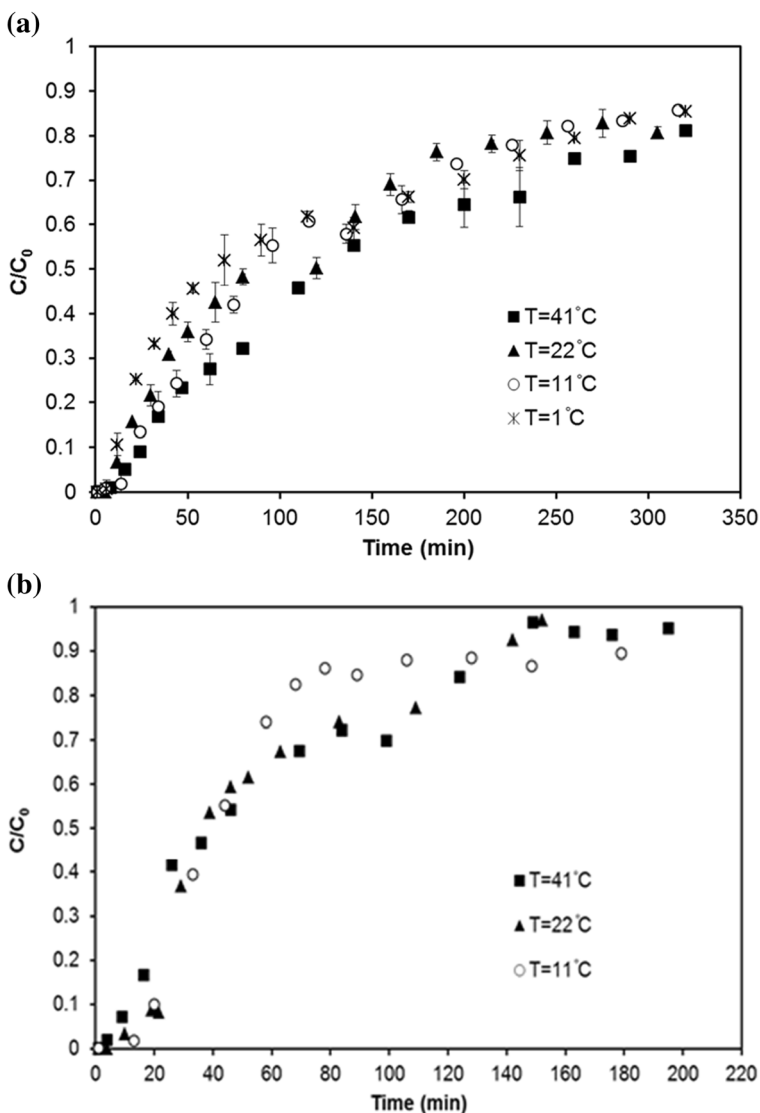
Fig. 4 Breakthrough curves for H_2S adsorption on 18 and 80–200 nm ZnO. **a** 94.70 and 86.80 ppmv H_2S . **b** 1501.85 and 1523.55 ppmv H_2S . Gas flow rate = $200 \pm 0.2 \text{ mL min}^{-1}$. Temperature = $22 \pm 1 \text{ }^\circ\text{C}$. Error bars represent standard deviation associated with the data determined through repeated sampling and analysis



capacity at 1, 11, 22, and 41 $^\circ\text{C}$ were 1.0, 2.1, 1.0, and 2.3 $\text{mg H}_2\text{S (g adsorbent)}^{-1}$, respectively. With $1567.8 \pm 63.0 \text{ ppmv H}_2\text{S}$, a decrease in the breakthrough capacity was observed due to increases in temperature, with the calculated values at 11, 22, and 41 $^\circ\text{C}$ being 7.3, 6.7, and 2.9 $\text{mg H}_2\text{S (g adsorbent)}^{-1}$, respectively. Regardless of H_2S concentration in the feed gas, the equilibrium adsorption capacity was not affected by the increase of temperature in the range 1 to 22 $^\circ\text{C}$ but increased slightly when a temperature of 41 $^\circ\text{C}$ was applied. For instance with $541.4 \pm 4.3 \text{ ppmv H}_2\text{S}$, the equilibrium adsorption capacities at 1, 11, and 22 $^\circ\text{C}$ were 17.4, 19.9, and 18.8 $\text{mg H}_2\text{S (g adsorbent)}^{-1}$, respectively, while a higher value of 26.1 $\text{mg H}_2\text{S (g adsorbent)}^{-1}$ was obtained at 41 $^\circ\text{C}$. A less

drastic effect was observed with $1567.8 \pm 63.0 \text{ ppmv H}_2\text{S}$ where equilibrium adsorption capacities at 11, 22, and 41 $^\circ\text{C}$ were 26.1, 25.2, and 27.7 $\text{mg H}_2\text{S (g adsorbent)}^{-1}$, respectively. Wang et al. (2008) investigated the chemisorption of H_2S by ZnO nanoparticles supported on mesoporous silica SBA-15 at room temperature and atmospheric pressure. The highest H_2S uptake at the breakthrough point was 100 $\text{mg H}_2\text{S (g adsorbent)}^{-1}$ and achieved with the adsorbent that contained 1.2 wt% zinc. These authors attributed the ZnO and H_2S reaction in a thin hydrated lattice of metal oxide as the main mechanism for the capture of H_2S . Nassar and Pereira-Almao (2010) investigated the sorption of H_2S by in situ prepared colloidal metal oxides in an oil sand matrix. The evaluated metal

Fig. 5 Breakthrough curves for H_2S adsorption on 18 nm ZnO at various temperatures. **a** 541.4 ± 4.3 ppmv H_2S . **b** 1567.8 ± 63 ppmv H_2S . Gas flow rate = 200 ± 0.2 mL min^{-1} . Error bars represent standard deviation associated with the data determined through repeated sampling and analysis



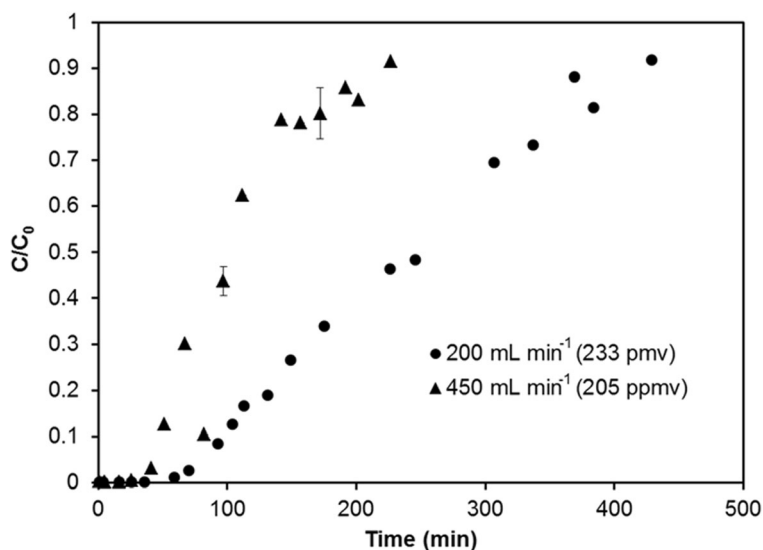
oxides included ZnO and those which are commonly used in upgrading of heavy oil (i.e., CuO, NiO, and Al_2O_3). With ZnO, an increase of temperature in the range 25 to 200 $^\circ\text{C}$ decreased the slope of the breakthrough curves and led to longer breakthrough times. The level of adsorbed H_2S at the breakthrough point was reported to be similar for all evaluated metal oxides. Habibi et al. (2010) observed a slight decrease in breakthrough adsorption capacity of rod-shaped ZnO nanoparticles due to a decrease of temperature from 250 to 150 $^\circ\text{C}$. The breakthrough adsorption capacity of rod-like ZnO nanoparticle at 250 and 150 $^\circ\text{C}$ was reported as 240 and 200 mg H_2S (g adsorbent) $^{-1}$, respectively. Other studies, however, have indicated a decrease in the breakthrough adsorption capacity of

ZnO with increases of temperature from 300 to 400 $^\circ\text{C}$ (Novochinskii et al. 2004). The variation in characteristics of ZnO nanoparticles and experimental conditions, specially applied temperatures, could explain the differences in the observed effect of temperature and adsorption capacities reported in various works.

3.3 Effect of Gas Flow Rate

Results for adsorption of H_2S on 18 nm ZnO particles with gas flow rates of 200 ± 0.2 and 450 ± 0.3 mL min^{-1} at 22 ± 1 $^\circ\text{C}$ are presented in Fig. 6. Increase in gas flow rate from 200 ± 0.2 to 450 ± 0.3 mL min^{-1} reduced the breakthrough time from 80 to 41 min and led to a steeper

Fig. 6 Breakthrough curves for H_2S adsorption on 18 nm ZnO nanoparticles at gas flow rates of 200 ± 0.2 and $450 \pm 0.3 \text{ mL min}^{-1}$. Temperature = $22 \pm 1 \text{ }^\circ\text{C}$. Error bars represent standard deviation associated with the data determined through repeated sampling and analysis



breakthrough curve, indicating that adsorbent reached its saturation stage faster when a higher gas flow rate was applied. Both breakthrough and equilibrium adsorption capacities decreased due to an increase of gas flow rate as a consequence of shorter gas residence time, with the values of breakthrough capacities at flow rates of 200 ± 0.2 and $450 \pm 0.3 \text{ mL min}^{-1}$ being 5.1 and 2.7 mg H_2S (g adsorbent)⁻¹, respectively. The corresponding equilibrium capacities were 16.1 and 7.8 mg H_2S adsorbed (g adsorbent)⁻¹, respectively. Decreasing trend in adsorption capacity as a result of increase in gas flow rate has been reported in earlier works with ZnO particles (Novochinskii et al. 2004; Habibi et al. 2010). Using 0.05–3 mm ZnO particles with Ca-bentonite as the binder for adsorption of 1–10 ppbv H_2S at 300 °C, Novochinskii et al. (2004) reported a decrease in adsorption capacity from 4.2 to 1.4 mg H_2S adsorbed (g adsorbent)⁻¹ as a result of increase in gas space velocity from 2659 to 8775 h⁻¹. Habibi et al. (2010) used rod-shaped ZnO nanoparticles (64 × 283 nm) to evaluate the effect of space velocities on adsorption of 5000–10,000 ppmv H_2S at 150–250 °C and reported that adsorption capacity decreased from 240 to 115 mg H_2S (g adsorbent)⁻¹ when space velocity was increased in the range 4000–8000 h⁻¹.

3.4 Adsorption Isotherms

As described in Section 2.6, equilibrium adsorption capacities and corresponding gas phase H_2S concentrations (partial pressures) were fitted into Langmuir, Freundlich,

and Langmuir-Freundlich isotherms. The goodness of fit for these isotherms for three sets of data (i.e., 10 and 22 °C for 18 nm ZnO and 22 °C for 80–200 nm ZnO) are compared in Fig. 7 and the associated coefficients are summarized in Table 1. Data presented in Fig. 7 reveal that regardless of particle size and temperature equilibrium adsorption capacity increased as gas phase H_2S concentration was increased. At a constant temperature, a decrease in the adsorbent particle size led to higher H_2S concentration in the solid phase. Finally, an increase of temperature from 10 to 22 °C did not have a marked effect on equilibrium adsorption capacity. A comparison of the regression coefficients listed in Table 1 indicated that Langmuir-Freundlich matched the experimental data obtained with various particle sizes and temperatures with a higher level of accuracy when compared with Langmuir and Freundlich isotherms. Haimour et al. (2005) investigated the removal of dissolved H_2S from acidic solutions at 25 and 35 °C using commercial ZnO particles. These authors reported equilibrium adsorption capacities of 30 and 45 g H_2S (g adsorbent)⁻¹ at 25 and 35 °C, respectively. Fitting the experimental data into various adsorption isotherms, Haimour et al. (2005) reported that compared with Langmuir and Freundlich, Redlich-Peterson isotherm was more accurate in predicting the experimental data.

3.5 Treatment of Swine Manure Gas in Semi-Pilot Scale Adsorption System

Figure 8a shows H_2S concentration profiles in the feed and treated gas streams during the first set of experiments in

Fig. 7 Equilibrium isotherms evaluated for adsorption of H₂S on ZnO nanoparticles. *Symbols* represent the experimental data at 10 and 22 °C for 18 nm particles and at 22 °C for 80–200 nm particles. *Lines* represent the goodness of fit for Langmuir (a), Freundlich (b), and Langmuir-Freundlich (c) isotherms

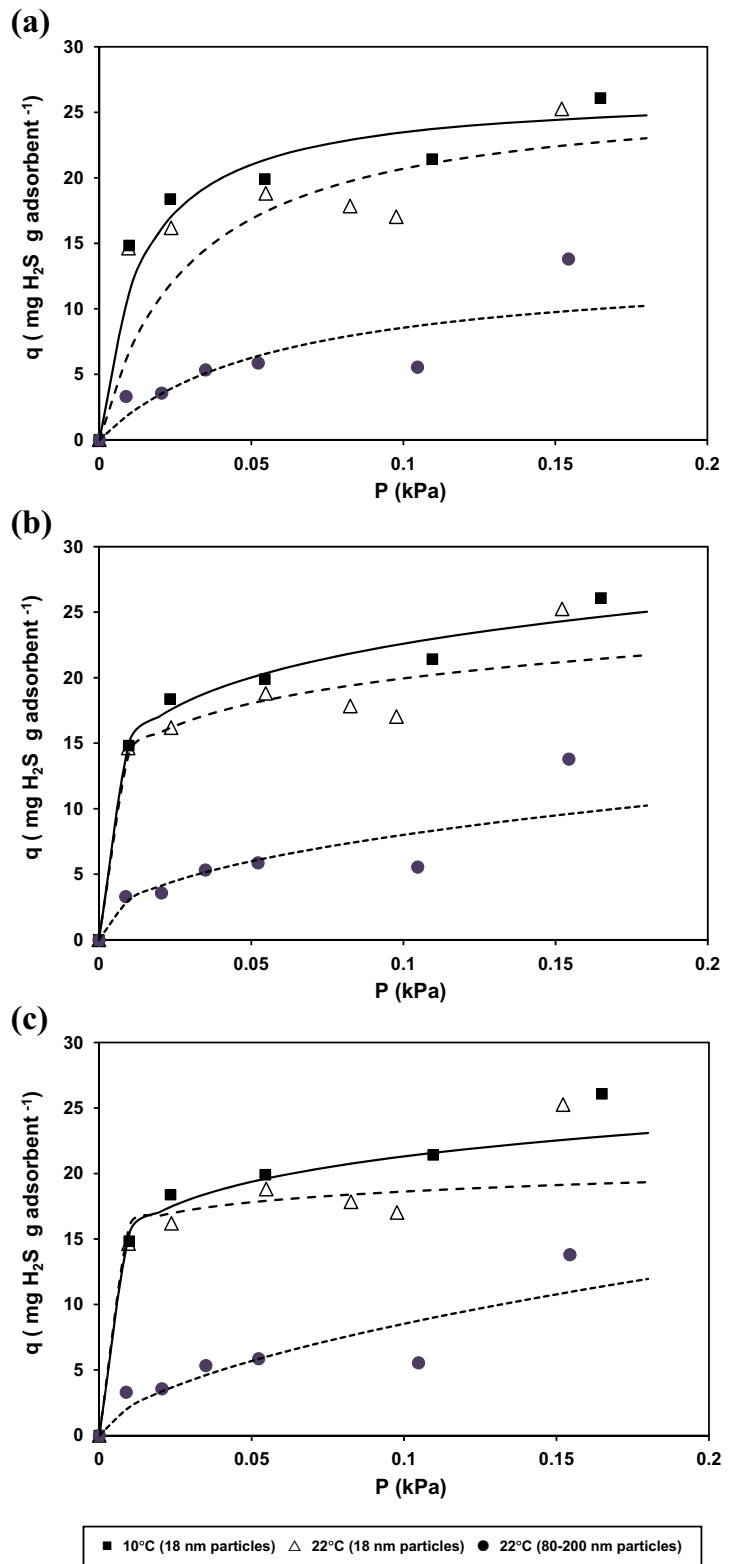


Table 1 Coefficients of various isotherms evaluated for adsorption of H₂S by ZnO nanoparticles

Isotherm	Temperature (°C)	Particle size (nm)	q_s (mg H ₂ S g adsorbent ⁻¹)	k	n	R^2
Langmuir	10	18	26.6	75	–	0.998
	22	18	26.8	33.9	–	0.862
	22	80–200	13.5	17.2	–	0.541
Freundlich	10	18	–	33.7	5.7	0.936
	22	18	–	27.8	6.9	0.635
	22	80–200	–	21.1	2.4	0.753
Langmuir-Freundlich	10	18	550	0.056	7	0.920
	22	18	599	0.037	15	0.882
	22	80–200	180	0.202	1.6	0.813

which semi-pilot scale adsorption column was fed continuously with manure gas for an extended period of 100 min (i.e., five consecutive cycles). As expected, due to variation in the extent of anaerobic digestion and the level of accumulated H₂S in each container, fluctuation in the H₂S content of manure gas was observed, with the lowest and the highest initial H₂S concentrations in the manure gas being 139.9 and 366.6 ppmv, respectively (average concentration = 235.7 ± 85.2 ppmv H₂S). As seen in the feed gas H₂S concentration profile (Fig. 8a), the experimental approach used in this work resulted in typical H₂S concentration profiles that occur in livestock facilities during handling of manure whereby high levels of H₂S are experienced initially and for a short time. This was followed by a decreasing trend in H₂S concentration due to depletion of H₂S content of manure and ventilation. To be more specific in the first cycle, feed gas H₂S concentration had an initial value of 238.4 ppmv that decreased to 90.4 ppmv after 12 min of withdrawing the gas from the headspace of manure container. Similarly in the third cycle, the feed gas H₂S concentration decreased from an initial value of 248.5 to 48.9 ppmv after 15 min of operation. Monitoring the concentration of H₂S in the treated gas revealed that ZnO nanoparticles effectively removed the H₂S from the manure gas and the level of H₂S in the treated gas in all five cycles was negligible (H₂S concentration < 0.3 ppmv), even when the feed H₂S concentration was at the highest level of 366.7 ppmv. Results of the second experimental run, conducted 2 weeks after the first run, are also shown in Fig. 8b. The maximum concentration of H₂S in the manure gas was lower than that observed in the first run (186.3 vs 366.7 ppmv), which again point to inherent variation in the extent of anaerobic digestion and the level of accumulated H₂S in the manure containers. Similar to the first run,

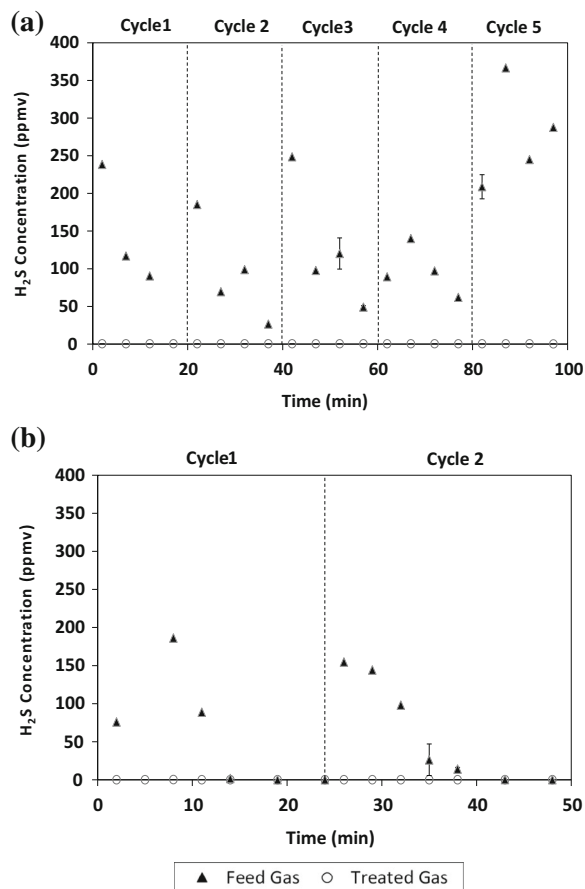


Fig. 8 H₂S concentration profiles in the swine manure gas (influent) and gas treated in semi-pilot scale adsorption system (effluent). **a** First experimental run with fresh 18 nm ZnO nanoparticles. **b** Second experimental run with exposed ZnO nanoparticles (100 h exposure to gases emitted from manure). Error bars represent the standard deviation of data determined by duplicate sampling

Table 2 Summary of the recent data published on adsorption of H₂S by ZnO particles

Reference	Adsorbent type	Adsorbent size (nm)	Temperature (°C)	H ₂ S concentration (ppmv)	Gas flow rate (mL min ⁻¹)	Breakthrough adsorption capacity (mg H ₂ S g adsorbent ⁻¹)
Rosso et al. (2003)	ZnO300 (combustion synthesis; calcination at 300 °C)	$(2.5-4.5) \times 10^5$	250	100	400	33.5
	ZnO400 (combustion synthesis; calcination at 400 °C)	$(2.5-4.5) \times 10^5$	250	100	400	26.1
	ZnO500 (combustion synthesis; calcination at 500 °C)	$(2.5-4.5) \times 10^5$	250	100	400	1.2
	ZnO600 (combustion synthesis; calcination at 600 °C)	$(2.5-4.5) \times 10^5$	250	100	400	0.6
	ZnO _u 500 (urea method; calcination at 500 °C)	$(2.5-4.5) \times 10^5$	250	100	400	0.3
	ZnO _u 700 (urea method; calcination at 700 °C)	$(2.5-4.5) \times 10^5$	250	100	400	0.3
	ZnO (commercial)	–	250	100	400	5.3
Novochinskii et al. (2004)	ZnO sorbent (extrudate)	3×10^6	300	8	200–500	4.2
	ZnO sorbent (grains)	$(1.5-2.5) \times 10^5$	300	8	200–500	28.7
	ZnO sorbent (grains)	$(1.1-1.5) \times 10^5$	300	8	200–500	29.9
	ZnO sorbent (grains)	$(0.5-0.75) \times 10^5$	300	8	200–500	22.7
	ZnO sorbent (grains)	$(1.1-1.5) \times 10^5$	350	8	200–500	15.5
	ZnO sorbent (grains)	$(1.1-1.5) \times 10^5$	375	8	200–500	10.8
	ZnO sorbent (grains)	$(1.1-1.5) \times 10^5$	400	8	200–500	5.2
Habibi et al. (2010)	ZnO nanoparticles (spherical)	56	150–250	5000–10,000	1100	30.4–92.5
	ZnO nanoparticles (rod)	64×283	150–250	5000–10,000	1100	57.0–240.1
Wang et al. (2008)	Mesoporous silica SBA-15 supported ZnO nanoparticles (0.5% Zn)	–	25	1000	500	36.7
	Mesoporous silica SBA-15 supported ZnO nanoparticles (1.2% Zn)	–	25	1000	500	95.0
	Mesoporous silica SBA-15 supported ZnO nanoparticles (3.1% Zn)	–	25	1000	500	436.0
	Mesoporous silica SBA-15 supported ZnO nanoparticles (4.4% Zn)	–	25	1000	500	49.9
	Mesoporous silica SBA-15 supported ZnO nanoparticles (9.0% Zn)	–	25	1000	500	38.9
Song et al. (2013)	ZnO nanoparticles	–	Ambient	255	284	9.4
	Carbon nanotube supported ZnO nanoparticles (prepared by reflux reduction)	–	Ambient	255	284	17.4
	Carbon nanotube supported ZnO nanoparticles (prepared by microwave assisted reduction)	–	Ambient	255	284	31.7
	Graphite oxide supported ZnO nanoparticles (prepared by reflux reduction)	–	Ambient	255	284	50.1
	Graphite oxide supported ZnO nanoparticles (prepared by microwave-assisted reduction)	–	Ambient	255	284	120.5

Table 2 (continued)

Reference	Adsorbent type	Adsorbent size (nm)	Temperature (°C)	H ₂ S concentration (ppmv)	Gas flow rate (mL min ⁻¹)	Breakthrough adsorption capacity (mg H ₂ S g adsorbent ⁻¹)
Present work	ZnO nanoparticles	18	1	548	200	1.0
		18	11	97–1627	200	0.8–7.3
		18	22	95–1502	200	3.5–6.7
		18	41	540–1574	200	2.3–2.9
		80–200	22	87–1524	200	0.1–0.5

passing the manure gas through the adsorption column led to effective capture of H₂S and as reflected in Fig. 8b the level of H₂S in the treated gas in both cycles was negligible. Finally, control experiment conducted with manure gas in the absence of ZnO nanoparticles indicated that the extent of H₂S adsorption by components of the experimental system was less than 15%.

4 Discussion

Hydrogen sulfide is a toxic and corrosive gas with adverse effects on human and animal health and the environment. Synthesized nanoparticles supported by various matrices and to a lesser extent metal oxide nanoparticles such as ZnO have been evaluated in a number of works aiming to control emission of H₂S. Table 2 presents an overview of the recent works on removal of H₂S from gaseous streams using micron- and nano-sized ZnO-based adsorbents. Data compiled in this table include particles type and size, H₂S concentration, gas flow rate, applied temperature, and reported breakthrough adsorption capacities. It should be noted that most of the works listed in this table did not provide detailed data on equilibrium adsorption capacities; thus, this information was not included. A close look at the data compiled in Table 2 reveals significant variations in the characteristics of ZnO particles used in different works (i.e., various sizes, supported vs unsupported, and different preparation techniques), as well as varied experimental conditions (i.e., differences in applied H₂S concentration, gas flow rate, and temperature). These variations make the direct comparison of these works somewhat impractical and could be considered as one of the reasons for substantial variations in the reported

breakthrough adsorption capacities. Nevertheless, one could evaluate the provided data in terms of applied temperatures and particle sizes and establish relevant patterns. For instance, the breakthrough capacities reported for micron-sized ZnO (Rosso et al. 2003; Novochinskii, et al. 2004) vary in the range 0.3–33.5 mg H₂S (g adsorbent)⁻¹, while higher values ranging from 30.4 to 240.1 mg H₂S (g adsorbent)⁻¹ have been reported for the nanoparticles (Habibi et al. 2010; Song et al. 2013). Comparison of the data for specially tailored ZnO nanoparticles with various supports such as silica, carbon, or graphite (Wang et al. 2008; Song et al. 2013) and unsupported ZnO nanoparticles (Song et al. 2013; present work) at ambient temperature range points to higher adsorption capacities for the tailored and/or supported adsorbent (17.4–436.0 vs 2.3–9.4 mg H₂S (g adsorbent)⁻¹). Although specially designed ZnO adsorbents could offer higher adsorption capacities when compared with pure metal oxide, the use of metal oxides that are effective, accessible, and easy to implement could be a preferred and feasible option for applications such as control of hydrogen sulfide emissions from livestock operations and for the treatment of biogas. A review of the recent literature also indicates that information regarding the application of ZnO nanoparticles as an adsorbent for capture of H₂S from the gases emitted from livestock facilities and biogas is very limited. In fact, earlier efforts on application of nanoparticles for mitigating hazardous emissions from livestock operations have focused exclusively on direct addition of ZnO or other nanoparticles to the manure as a means to inhibit microbial activity and formation of H₂S and ammonia in the manure (Alvarado et al. 2015; Gautam, et al. 2016). Thus, the present work appears to be one of the first that reports on the use of ZnO nanoparticles for

the treatment of gases emitted from swine manure that also provides detailed information on performance of this adsorbent under a wide range of conditions, especially at the ambient temperatures that are likely to prevail in the livestock operations.

5 Conclusions

The results of the current study indicated that adsorption of H₂S by ZnO nanoparticles was influenced by concentration of H₂S, gas flow rate, particle size, and to a lesser extent temperatures in the ambient range. The adsorption rate and capacities increased with increases of H₂S concentration, though the effect was more pronounced for the lower concentration range. Similarly, the decrease in particle size from 80 to 200 nm to 18 nm led to higher adsorption capacities. The increase of gas flow rate shortened the residence time and led to lower adsorption capacities. Regardless of H₂S concentration, the equilibrium adsorption capacity was not affected by variation of temperature in the range 1 to 22 °C but increased slightly when temperature increased to 41 °C. Among the evaluated isotherms, Langmuir-Freundlich described the equilibrium data with a higher level of accuracy. Experiments conducted in the semi-pilot scale adsorption system with gases emitted from the stored swine manure confirmed the effectiveness of ZnO nanoparticles in capture of H₂S from the gases representing emissions from livestock facilities. Overall, the results of the present study demonstrate that an adsorption system utilizing ZnO nanoparticles could offer an effective approach for control of H₂S emission in applications where an accessible and easy to use adsorbent is required.

Acknowledgements This work was made possible through the financial support of the Agriculture and Agri-Food Canada through the Canadian Agricultural Adaptation Program (CAAP) delivered by the Agriculture Council of Saskatchewan and the Saskatchewan Pork Development Board. Financial support provided to MN by the Natural Science and Engineering Council of Canada is gratefully acknowledged.

References

Alvarado, A. C., Predicala, B. Z., & Asis, D. A. (2015). Mixing nanoparticles with swine manure to reduce hydrogen sulfide

- and ammonia emissions. *International journal of Environmental Science and Technology*, *12*, 893–904.
- Arogo, J., Zhang, R. H., Riskowski, G. L., & Day, D. L. (2000). Hydrogen sulfide production from stored liquid swine manure: a laboratory study. *ASAE Transaction*, *43*, 1241–1245.
- Chang, D.L., Lee, S.J., Choi, W.Y. & Lee, K.S. (2004). A pilot scale biofilter system to reduce odour from swine operation. Paper presented at *ASAE/CSAE Annual International Meeting*; Ottawa, Ontario.
- Chénard, L., Lemay, S. P., & Laguë, C. (2003). Hydrogen sulfide assessment in shallow pit swine housing and manure storages. *Journal of Agricultural Safety Health*, *9*, 285–302.
- Chung, Y. C., Huang, C., Tseng, C. P., & Pan, J. R. (2000). Biotreatment of H₂S- and NH₃-containing waste gases by immobilized cells biofilter. *Chemosphere*, *41*, 329–335.
- Curtis, S. E. (1983). *Environmental management in animal agriculture*. Iowa: Iowa State University Press.
- Gautam, D. P., Rahman, S., Fortuna, A. M., Borhan, M. S., Saini-Eidukat, B., & Bezbaruah, A. N. (2016). Characterization of zinc oxide nanoparticle (nZnO) alginate beads in reducing gaseous emission from swine manure. *Environmental Technology*, *11*, 1–14.
- Habibi, R., Rashidi, A. M., Daryan, J. T., & Zahed, A. M. A. (2010). Study of the rod-like and spherical nano-ZnO morphology on H₂S removal from natural gas. *Applied Surface Science*, *257*, 434–439.
- Haimour, N., El-Bishtawi, R., & Ail-Wahbi, A. (2005). Equilibrium adsorption of hydrogen sulfide onto CuO and ZnO. *Desalination*, *181*, 145–151.
- Hartung, J., & Phillips, V. R. (1994). Control of gaseous emissions from livestock buildings and manure stores. *Journal of Agricultural Engineering Research*, *5*, 173–189.
- Kim, Y. K., Ko, H. J., Kim, H. T., Kim, Y. S., Roh, Y. M., Lee, C. M., & Kim, C. N. (2008). Odor reduction rate in the confinement pig building by spraying various additives. *Bioresource Technology*, *99*, 8464–8469.
- Li, L., & King, D. L. (2006). H₂S removal with ZnO during fuel processing for PEM fuel cell applications. *Catalysis Today*, *116*, 537–541.
- McCrory, D. F., & Hobbs, P. J. (2001). Additives to reduce ammonia and odor emissions from livestock wastes: a review. *Journal of Environmental Quality*, *30*, 345–355.
- Moreno, L., Predicala, B., & Nemati, M. (2010). Laboratory, semi-pilot and room scale study of nitrite and molybdate mediated control of H₂S emission from swine manure. *Bioresource Technology*, *101*, 2141–2151.
- Nassar, N. N., & Pereira-Almao, P. (2010). Capturing H₂S(g) by in situ-prepared ultra-dispersed metal oxide particles in an oil-sand-packed bed column. *Energy & Fuels*, *24*, 5903–5906.
- Novochinskii, I. I., Song, C., Ma, X., Liu, X., Shore, L., Lampert, J., & Farrauto, R. J. (2004). Low-temperature H₂S removal from steam contacting gas mixtures with ZnO for fuel cell application. 1. ZnO particles and extrudates. *Energy & Fuels*, *18*, 576–583.
- Predicala, B., Nemati, M., Stade, S., & Lague, C. (2008). Control of H₂S emission from swine manure using Na-nitrite and Na-molybdate. *Journal of Hazardous Materials*, *154*, 300–309.
- Rosso, I., Galletti, C., Bizzi, M., Saracco, G., & Specchia, V. (2003). Zinc oxide sorbents for the removal of hydrogen

- sulfide from syngas. *Industrial & Engineering Chemistry Research*, 42, 1688–1679.
- Sayyadnejad, M. A., Ghaffarian, H. R., & Saeidi, M. (2008). Removal of hydrogen sulfide by zinc oxide nanoparticles in drilling fluid. *International Journal of Science and Technology*, 5, 565–569.
- Shah, S. B., Westerman, P. W., Munilla, R. D., Adcock, M. D., & Baughtman, G. R. (2008). Design and evaluation of a regenerating scrubber for reducing animal house emissions. *Transaction of ASABE*, 51, 243–250.
- Simo, M., Sivashanmugam, S., Brown, C. J., & Hlavacek, V. (2009). Adsorption/desorption of water and ethanol on 3A zeolite in near-adiabatic fixed bed. *Industrial & Engineering Chemistry Research*, 20, 9247–9260.
- Song, H. S., Park, M. G., Kwon, S. J., Yi, K. B., Croiset, E., Chen, Z., & Nam, S. C. (2013). Hydrogen sulfide adsorption on nano-sized zinc oxide/reduced graphite oxide composite at ambient condition. *Applied Surface Science*, 276, 646–652.
- Tang, K., Baskaran, V., & Nemati, M. (2009). Bacteria of the sulphur cycle: an overview of microbiology, biokinetics and their role in petroleum and mining industries. *Biochemical Engineering Journal*, 44, 73–94.
- Thu, K. M. (2002). Public health concerns for neighbours of large-scale swine production operations. *Journal of Agricultural Safety and Health*, 8, 175–184.
- Tien, C. (1994). *Adsorption calculations and modeling*. Newton: Butterworth-Heinemann.
- Wang, X., Sun, T., Yang, J., Zhao, L., & Jia, J. (2008). Low-temperature H₂S removal from gas streams with SBA-15 supported ZnO nanoparticles. *Chemical Engineering Journal*, 142, 48–55.
- Xiao, Y., Wang, S., Wu, D., & Yuan, Q. (2008). Experimental and simulation study of hydrogen sulfide adsorption on impregnated activated carbon under anaerobic conditions. *Journal of Hazardous Materials*, 153, 1193–1200.